MULTI-DEGREE-OF-FREEDOM DYNAMIC WIND-TUNNEL TESTING OF A DELTA WING USING A ROBOTIC MANIPULATOR

Keisuke ASAI*, Atsushi KONNO*, Xin JIANG*, Daiju NUMATA*, Hiroyuki ABE*, Nobuhiro NAKATA*, and Tatsuya HARA*
***Graduate School of Engineering, Tohoku University, Sendai, Japan**
asai@aero.mech.tohoku.ac.jp

Keywords: *Dynamic Wind-Tunnel Testing, Multi-Degree-of-Freedom, Robotic Manipulator, Delta Wing, Vortex Breakdown*

Abstract

The purpose of this study is to measure the unsteady force acting on a slender delta wing in two degree-of-freedom (DoF) motion. A serial-type robot manipulator was used to oscillate the model in two modes; one is roll-yaw coupled lateral motion and the other is pitch-heave coupled longitudinal motion. Unsteady forces and moments were measured by a six-component balance and the effects of oscillation frequency and amplitude were evaluated. In the 2-DoF roll-yaw coupled mode, hysteresis loop was noted at high angles of attack and changes of rolling moment are delayed as compared with the 1-DoF case. In the pitch-heave coupled experiment, it was found that the effect of pitch rate on unsteady force is negligible at the frequency and amplitude ranges covered in this experiment.

1 Introduction

The increasing agility and maneuver capabilities of micro air vehicles (MAVs) have posed a challenging problem on aircraft stability and control. The conventional linear theory based on stability derivatives might not be valid for the flight region at high angles of attack where the flow on the vehicle is highly separated and exhibits nonlinear (and/or unsteady) aerodynamic characteristics such as hysteresis, dynamic stall, rocking oscillation and so on [1-4]. In addition, in such extreme flight conditions, the motion of aircraft is inherently multi-directional so each degree-of-freedom cannot be treated separately. This means that dynamics of those vehicles has to be treated as multi-degree-of-freedom problems such as roll-yaw and pitch-heave combined motions.

Recently, the studies on multiple-degrees of freedom motion has been becoming possible using robotic devices like the link mechanism at Tottori University [5] and the Model Positioning Mechanism (MPM) at DLR [6]. These robotic manipulators can cover a wide range of frequency and amplitude.

In this study, a multi-degree-of-freedom dynamic wind-tunnel testing has been conducted to evaluate dynamic behaviors of a delta wing model at high angles of attack [7,8]. To accomplish arbitrary multi-DOF model motion, a serial-type robotic manipulator has been introduced. A slender delta wing model with sweep angle of 80 deg was tested in two different 2-DoF modes: one is roll-yaw-coupled lateral motion and the other is pitch-heave coupled longitudinal motion. The latter allows us to separate the effects of angle-of-attack derivative $\dot{\alpha}$ and pitch rate q on dynamic stability of the model.

In this experiment, unsteady force and moment were measured by a six-component balance and effects of oscillation frequency and amplitude were studied over a wide range of frequency and amplitude. From the results obtained by experiment, the relationship between high-angle of attack characteristics of the slender delta wing and unsteady flow field in 2-DoF motions is discussed.

2 Description of Experiment

2.1 Robotic Manipulator

An intelligent serial-type robot manipulator (PA-10, Mitsubishi Heavy Industries, Ltd.) was used for to produce a multi-DoF motion of the model (Fig. 1). This manipulator consists of seven actuators that can be operated independently. Maximum angular speed is 2π rad/sec for a motor at the tip and 1 rad/sec for the other motors, allowing us to oscillate the model fast enough for unsteady effects to dominate. In the case of 2-DoF roll-yaw coupled motion (Fig. 2(a)), the yawing motion was generated by moving six motors based on inverse kinematics. On the other hand, in the case of 2-DoF pitch-heave coupled motion, the manipulator was installed at the side of the test section. A pitch oscillation rig shown in Fig. 2(b) was used to produce sinusoidal pitching motion.

2.2 Test Model

The model used in this study is a simple flat-plate model with the sweep angle of 80 degrees. The length (c) is 300 mm and the thickness (h) is 2 mm. The leading-edge is sharp and truncated at 45 deg. The model was mounted on the tip of the manipulator.

2.3 Wind Tunnel

Experiments were conducted in the Low-Turbulence Wind Tunnel at Institute of Fluid Science (IFS), Tohoku University. This is a closed circuit wind-tunnel with the open-type test section with the cross distance of 0.8 m. Additionally, flow visualization tests on the delta wing were conducted in the IFS's blown-type low-speed tunnel at ISF having a nozzle with 0.8-m square cross section.

2.3 Test condition

In this experiment, we studied two different types of 2-DoF oscillation modes; one is roll-yaw coupled lateral motion and the other is pitch-heave coupled longitudinal motion. A particular emphasis has been placed on the effects of the frequency and amplitude of oscillation on dynamic stability.

In the roll-yaw experiment, the amplitude of rolling motion has been changed from 5 to 30 degrees while the yawing amplitude has been changed from 2.5 to 10 degrees. The oscillating frequency has been changed from zero to 1 Hz. This corresponds to the non-dimensional frequency ($k=fc/U_\infty$) range up to 0.01 for the free-stream velocity U_∞ of 30 m/sec and the model length c of 0.3 m. A phase angle between the roll and yaw motion was set at $\pi/2$ to simulate Dutch-roll like motion (Fig. 3). The angle of attack was changed from zero to 40 deg.

The pitch-heave experiment was conducted at the center angles of attack α_0 at 30 and 38 deg. The amplitude of effective angle of attack α_{eff} and that of pitch rate q were fixed at 3 deg. It was difficult to produce large amplitude oscillations because oscillation amplitude was restricted by the frequency performance of a manipulator. The oscillating frequency was set either at 0.6 and 0.9 Hz that correspond to the non-dimensional frequency ($k=fc/U_\infty$) of 0.024 and 0.036, respectively, for the free-stream velocity U_∞ of 7.5 m/sec and the model length c of 0.3 m. The phase angle between the pitch and heave motions was set at $\pi/2$ to produce pure pitching motion (Fig. 4).

Aerodynamic forces and moments were measured using a six-component load cell (IFS-90M31A50-150, Nitta Corp.) installed on the tip of the manipulator. The tare due to inertia of the model was measured under no-wind condition and subtracted from the measurement under wind-on condition to extract pure aerodynamic effects. To reduce the noise, the same measurement was repeated over 40 times. The obtained data were then ensemble averaged and filtered by a low-pass filter with the cut-off frequency at 15 Hz for roll-yaw experiment and at 3 Hz for pitch-heave experiment.

In the flow visualization experiment, the cross section of the leading-edge separation vortices was illuminated by a thin sheet of laser light produced by a 5 W Argon laser. A smoke generator was used to produce smoke. The laser sheet was set to illuminate the model at x/c = 0.5 and 1.0 (trailing edge) and the cross-sectional

images of vortex were recorded by a digital camera (IOS 7D, Canon Corp.) at 30 fps. In this experiment, the free-stream velocity U_∞ was set at 2 m/s to prevent a diffusion of the smoke and to have clearer vortex core images. It is noted that the vortex breakdown over slender, sharp-edged, delta wings are insensitive to Reynolds number [9].

3 Results and Discussion

3.1 Roll and yaw coupled motion

Aerodynamic behavior of a delta wings are determined by behavior of the leading-edge vortices [1, 10-13]. Figure 5 shows the observed boundaries of vortex symmetry/ asymmetry and burst for a delta wing [10]. Two specific boundaries are noted to distinguish vortex behaviors. These boundaries are determined by the effective angle of attack α_{eff} and the effective sweep angle Λ_{eff} given by the following equations;

$$\alpha_{eff} = \tan^{-1}(\tan\alpha\cos\phi)\cos\beta \qquad (1)$$

$$\Lambda_{eff} = 90 \pm \beta - (\theta \pm \tan^{-1}(\tan\alpha\sin\phi)) \qquad (2)$$

where ϕ is roll angle, β is side slip angle, and θ is pitch angle of the model.

Figure 6 shows the rolling moment of the 80-deg delta wing model for angles of attack from 15 to 40 deg, roll amplitude $\Delta\varphi$ = 30 deg, yaw amplitude $\Delta\beta$ = 5 deg, and k = 0.01 (f = 1 Hz). For comparison, the rolling moment in pure rolling motion (meaning 1-DOE motion) is shown as dashed line. As shown in Fig. 6, strong hysteretic characteristics appear at angles of attack higher than 35 degree.

Figure 7 shows a plot of roll damping coefficient given by

$$C_{\ell_p} = \frac{\partial C_\ell}{\partial \dfrac{pb}{2U_\infty}} = \frac{\partial C_\ell}{\partial p}\frac{2U_\infty}{b} \qquad (3)$$

As shown in Fig. 7, the rolling motion is damped as the roll angle approaches to maximum amplitude. This damping effect becomes much smaller in the 2-DOF case. In the 2-DoF cases, the rolling moment forms a counter-clockwise loop at low angles of attack that is attributed to the dihedral effects of sweep angle (stabilizing effect). At angles of attack higher than 35 deg, the rolling moment starts to form a clockwise loop in the range of small roll angle that will cause dynamic instability. In these conditions, energy is supplied from the free stream to the rolling wing.

The similar trend can be seen in Fig. 8 that shows the effects of yawing amplitude on rolling moment for α = 35 deg and $\Delta\varphi$ = 30 deg and k = 0.01 (f = 1 Hz). It is noted that the instability increases with increasing yawing amplitude.

Figure 9 shows the effects of roll amplitude on rolling moment, for α = 35 deg, $\Delta\beta$ = 5 deg and k = 0.01 (f = 1 Hz). It is noted that there is no indication of unsteadiness for $\Delta\varphi$ =5 deg and 10 deg, suggesting that a quasi-steady aerodynamic model is effective for oscillations with small amplitudes. For larger amplitudes, however, unsteady and nonlinear aerodynamic effects become dominant.

Figure 10 shows time variation of C_{roll} over one oscillation cycle. Plots of C_{roll}-ϕ relationship are also shown for comparison purpose. It is seen that there is time lag between the 2-DoF and 1-DoF (β = 0) cases for the leading-edge separation vortices to follow the moving wing surface. It is noted that, at α = 35 degree, the onset of vortex breakdown is delayed by an effect of yawing motion. This observation is also supported by the flow visualization experiments (Fig. 11). In the case of 2-DoF motion, detachment of the leading-edge vortices is delayed on the wing moving upward while the breakdown of the leading-edge vortices is delayed on the wing moving downward. For the 1-DoF oscillation, it takes $\Delta t/T$ = 0.46 for the vortex to recover from the breakdown. On the other hand, for the 2-DoF oscillation, it takes only $\Delta t/T$ = 0.35. This means that the yawing motion has an effect to delay vortex breakdown and promote its recovery.

Figure 12 shows the effects of DOF on the temporal locations of vortex breakdown and recovery in one oscillation cycle. It is noted that

behaviors of the leading-edge vortices are about the same between the 1-DoF and 2-DoF cases, when expressed in terms of effective angle of attack α_{eff} and effective sweep angle Λ_{eff} (Eqs. 1 and 2). These results suggest that the criteria based on α_{eff} and Λ_{eff} are valid even when the model is moving in 2-DoF mode.

3.2 Pitch and heave coupled motion

Unsteady delta-wing research has shown the normal force coefficients in pitching to overshoot or undershoot the static values. These unsteady phenomena are caused by the effect of pitch rate on breakdown of leading-edge vortices.

Figure 13 shows the static normal-force coefficients obtained when the model is pitched in the upward and downward directions. Hysteretic behavior is noted at angles of attack higher than 35 deg, suggesting an occurrence of vortex breakdown.

Considering dynamic pitching motion, the normal force coefficient acting on the model can be expressed by the following equation;

$$C_N = C_{N_0} + C_{N_\alpha}\alpha + C_{N_{\dot\alpha}}\dot\alpha + C_{N_q}q \qquad (4)$$

In simple pitch oscillation ($\theta = \Delta\theta\sin(2\pi f\cdot t)$), both $\dot\alpha$ and pitch rate q are changed with time. It is noted that the effects of these two parameters are inseparable. On the other hand, in simple heaving motion ($z = \Delta z\cdot\sin(2\pi f\cdot t)$) with a fixed pitch angle, a pure effect of the effective angle of attack can be obtained. A pure effect of pitch rate can be obtained by conducting a pitch-heave coupled oscillation. The phase between pitch and heave is set at $\pi/2$ to keep the effective angle of attack unchanged during the cycle.

Figure 14 compares the dynamic normal coefficients for pitching, heaving, and 2-DoF coupled motions for non-dimensional frequency of 0.024. Dynamic data are obtained for two different center angles of attack (α_0 = 30 and 38 deg). It is seen that, in the case of α_0 = 30 deg, the dynamic data does not show any hysteretic behavior, meaning there is no unsteady effect. On the other hand, for α_0 = 38 deg, dynamic hysteresis loop appears in pure pitching and heaving cases. Note here that hysteresis loop does not exist for 2-DoF tests, indicating that the effect of pitch rate on unsteady normal force is negligible at the frequency and amplitude range realized in this experiment. The same statement is valid for the case of k =0.036.

4 Concluding Remarks

A multi-degree-of-freedom dynamic wind-tunnel testing has been conducted to evaluate dynamic behaviors of a delta wing model at high angles of attack. To accomplish arbitrary multi-degree-of-freedom motions, a serial-type robotic manipulator has been introduced. In the present study, a slender delta wing model with sweep angle of 80 degree was tested in two different 2-DoF modes.

From the results in the roll-yaw experiment, it was found that the yawing motion has an effect to delay an onset of vortex breakdown, resulting in the time lag in unsteady rolling moment. On the other hand, from the pitch-yaw experiment, it was found that the effect of pitch rate on unsteady normal force is negligible in the frequency and amplitude range covered in this experiment.

To express behavior of a maneuvering delta wing at high angles of attack in more realistic manner, the unsteady effects have to be considered in modelling aerodynamic terms in the equation of motion. As demonstrated in the present study, multi-DoF robotic manipulators could be a useful device for dynamic wind-tunnel testing. However, a serial arm-type robotic manipulator has an inherent limitation of performance and speed that prevents us from evaluating the effects of oscillating frequencies and amplitudes over a wide range. A manipulator with parallel-link mechanism such as MPM and HEXA has much faster frequency performance and can be a solution to the present problem of serial robots.

Acknowledgement

The authors express their sincere thanks to Mr. Ota and Mr. Okuizumi for their technical support in wind-tunnel testing. The longitudinal 2-DoF tests were conducted as a part of graduation

project for Mr. D. Takayama. We'd like to acknowledge to his contribution to this paper. This work was supported by KAKENHI (22246103).

References

[1] Nelson R C, et al, "The unsteady aerodynamics of slender wing and aircraft undergoing large amplitude maneuvers", Progress in Aerospace Sciences Vol. 39, pp. 185-248 (2003)

[2] Greenwell D I, "A review of unsteady aerodynamic modelling for flight dynamics of manoeuvrable aircraft," AIAA Atmospheric Flight Mechanics Conference and Exhibit, Rhode Island, USA, AIAA-2004-5276 (2004)

[3] Huang X Z, et al., "Introduction and Experimental Aspects of The NATO RTO Task Group AVT-080: Study of Vortex Breakdown Over Slender Wings", European Congress on Computational Methods in Applied Sciences and Engineering ECCOMAS (2004)

[4] Cummings R M, et al, "An Integrated Computational/ Experimental Approach to UCAV Stability & Control Estimation: Overview of NATO RTO AVT-161", the 28th AIAA Applied Aerodynamics Conference, Chicago, IL, USA, AIAA-2010-4392 (2010)

[5] Kawazoe H, et al, "Ground Effect on the Dynamic Characteristics of a Wing-rock Delta Wing," the 34th AIAA Fluid Dynamics Conference and Exhibit, Portland, Oregon, USA, AIAA-2004-2352 (2004)

[6] Bergmann A, et al, "Experimental and numerical research on the aerodynamics of unsteady moving aircraft," Progress in Aerospace Sciences Vol. 44, pp.121-197 (2008)

[7] Abe H, "2-DoF Dynamic Wind-tunnel Testing of a Rolling Delta-wing Using a Robotic Manipulator," Master Thesis, Department of Aerospace Engineering, Tohoku University, March 2012 (2012)

[8] Takayama D, "2-DoF Dynamic Wind-tunnel Testing of a Pitching Delta-wing Using a Robotic Manipulator," Graduation Thesis, Tohoku University, March 2012 (2012)

[9] Lambert C and Gursul I, "Insensitivity of Unsteady Vortex Interactions to Reynolds Number," AIAA Journal, vol. 38, no. 5, pp. 937-939 (2000)

[10] Polhamus E C, "Predictions of Vortex Lift Characteristics by a Leading-Edge Suction Analogy", J. Aircraft, Vol. 8, p.193-1990 (1971)

[11] Shimbo Y and Sato J, "Unsteady Aerodynamic Forces on Rolling Delta Wings at High Angle of Attack," Trans. of the Japan Society for Aeronautical and Space Sciences, Vol. 37, No. 429 (1989)

[12] Kwak D Y, Sunada Y, Sato J, "Experimental Research on Unsteady Aerodynamics of Rolling Delta Wings," Trans. of the Japan Society for Aeronautical and Space Sciences, Vol. 45, No. 419 (1997)

[13] Gursul I, "Review of unsteady vortex flows over slender delta wings," Journal of Aircraft, 42 (2), pp. 299-319 (2004)

Copyright Statement

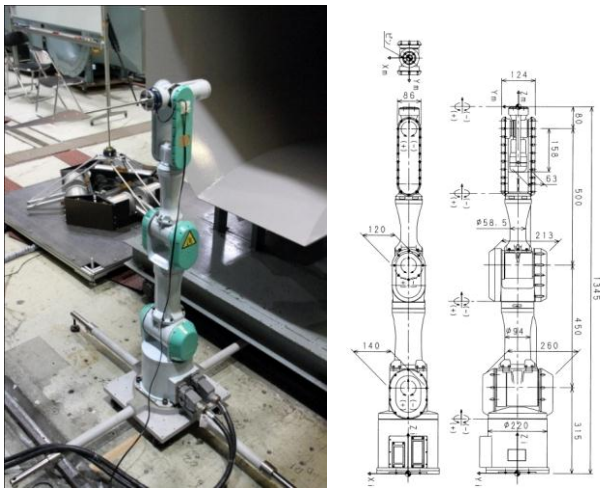

Fig. 1 Robotic manipulator

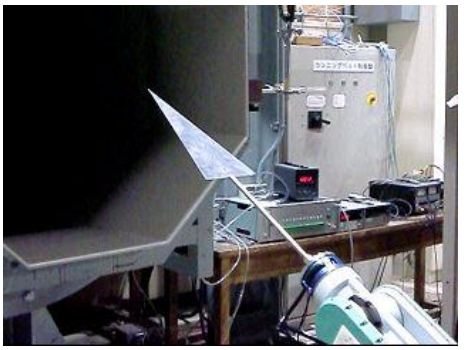

(a) roll and yaw

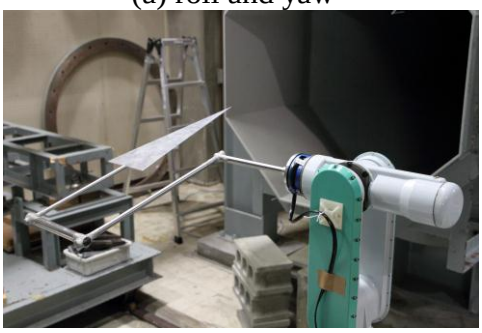

(b) pitch and heave

Fig. 2 Set-up for 2-DOF experiments

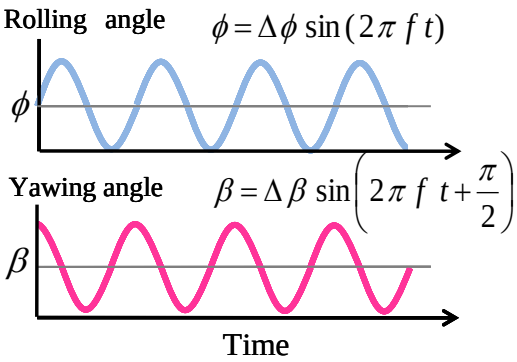

Fig. 3 Roll-yaw coupled mode

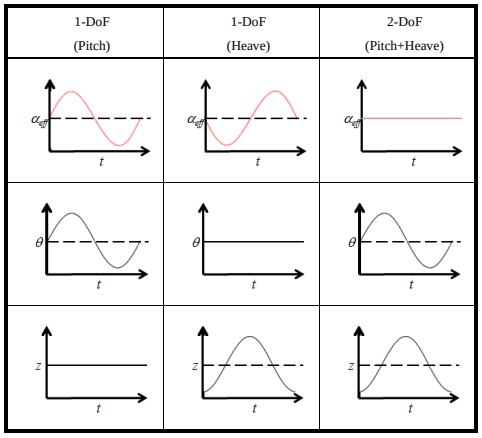

Fig. 4 Pitch-heave coupled mode

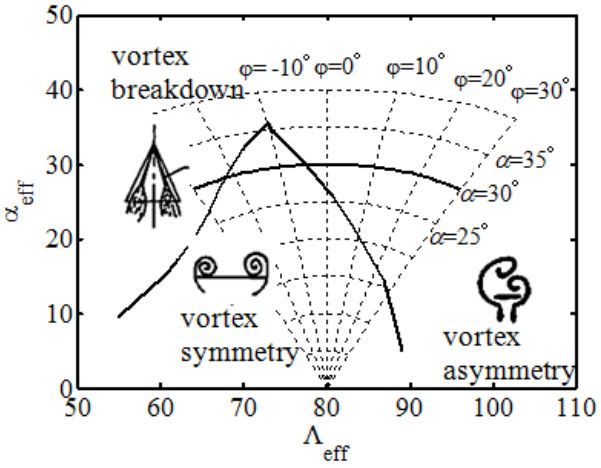

Fig. 5 Leading-edge vortex boundary for delta wings as a function of effective AoA and effective sweep angle

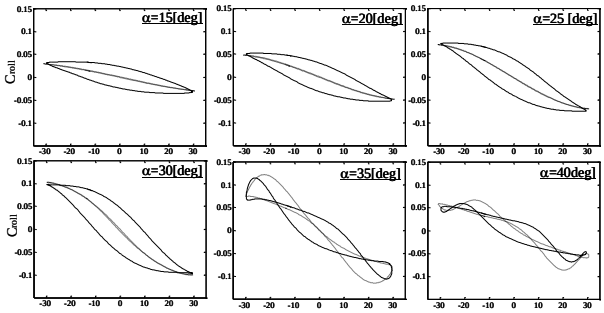

Fig. 6 Rolling moment in roll-yaw coupled motion for α from 15 to 40 deg, $\Delta\varphi$ = 30 deg, $\Delta\beta$ = 5deg, k = 0.01 (f = 1 Hz), dashed lines indicate data for 1-DoF ($\Delta\beta$ = 0 deg).

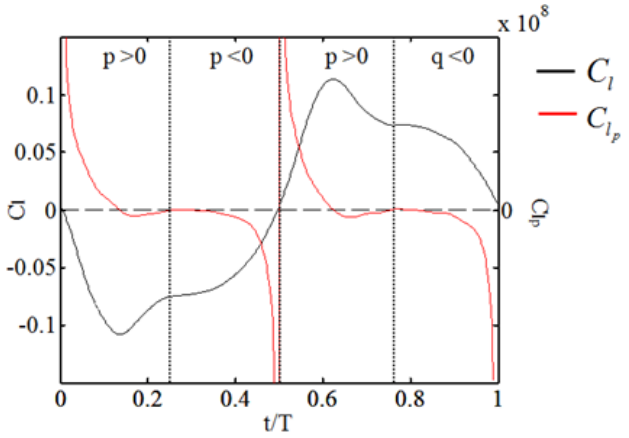

Fig. 7 Roll-dumpling coefficient

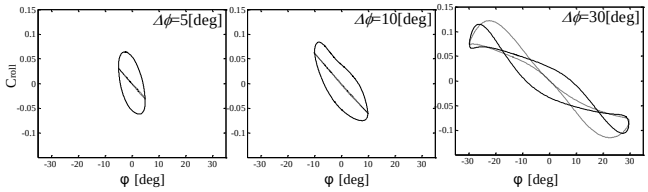

Fig. 8 Effects of roll amplitude on rolling moment in roll-yaw coupled motion, α = 35 deg, $\Delta\beta$ = 5 deg , k = 0.01 (f = 1 Hz), dashed lines indicate the data for $\Delta\beta$ = 0 deg.

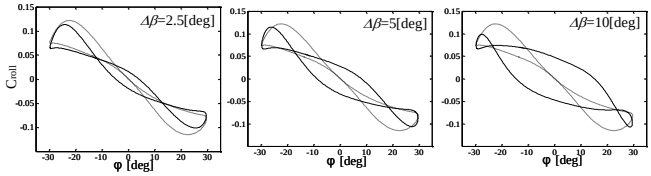

Fig. 9 Effects of yaw amplitude on rolling moment in roll-yaw coupled motion, α = 35 deg, $\Delta\varphi$ = 30 deg, k = 0.01 (f = 1 Hz), dashed lines indicate the data for $\Delta\beta$ = 0 deg.

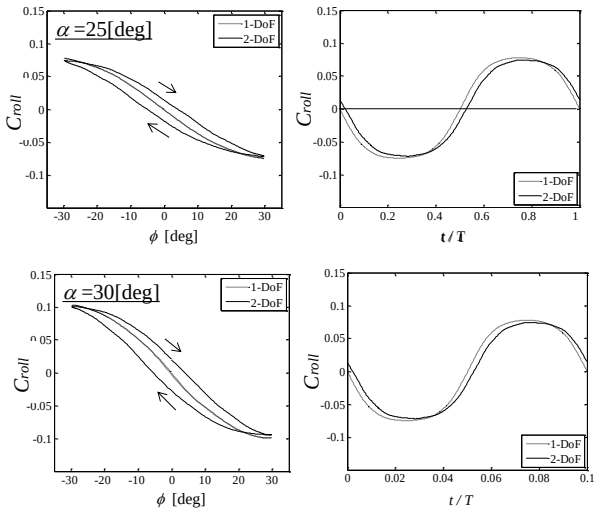

(continued)

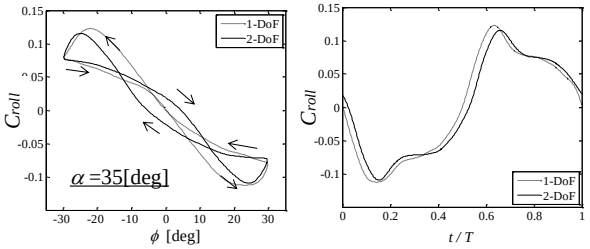

Fig. 10 Comparison of rolling-moment in 1-DoF and 2-DoF cases for α from 25 to 35 deg, $\Delta\varphi$ = 30 deg, k = 0.01 (f = 1 Hz), dashed lines indicate the data for 1-DoF.

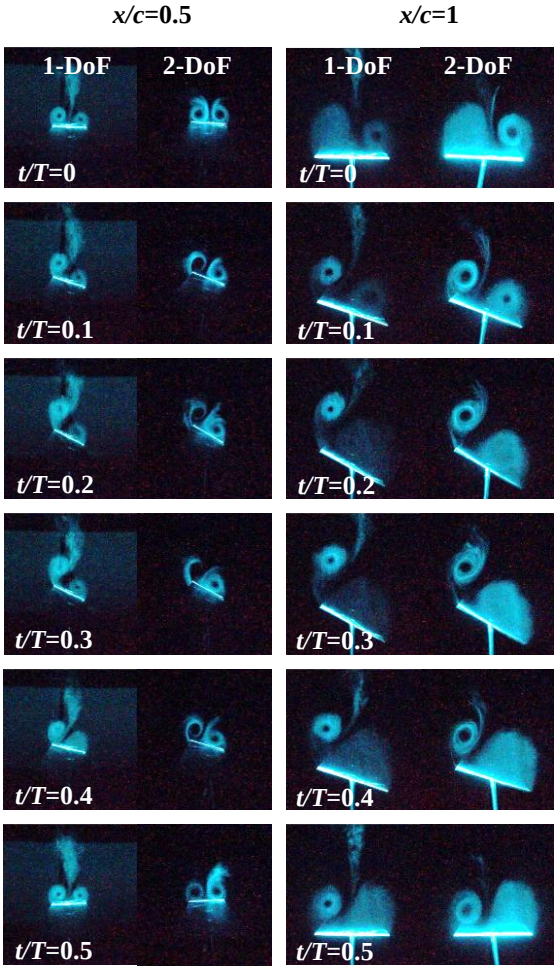

Fig. 11 Laser-light-sheet visualization of leading-edge vortices; a comparison between 1-DoF and 2-DoF cases

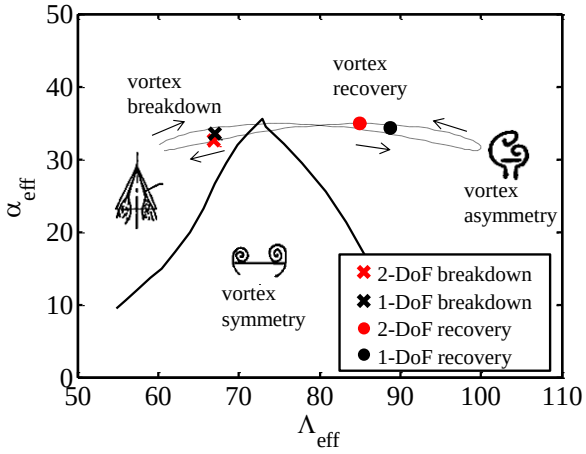

Fig. 12 Effect of yawing motion on breakdown and recovery of leading-edge vortices

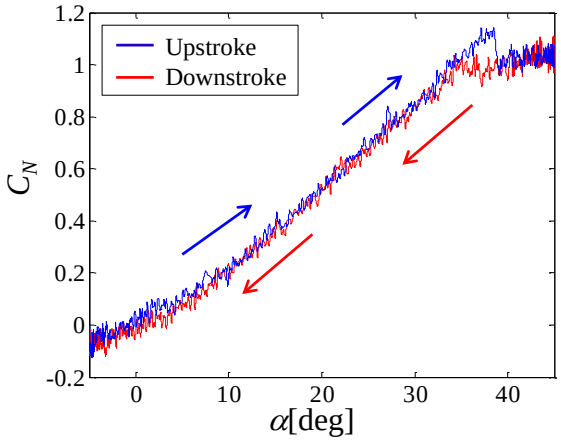

Fig. 13 Static normal force as a function of angle of attack,

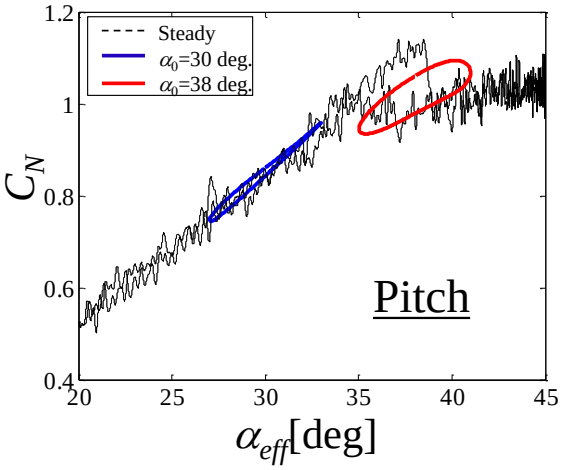

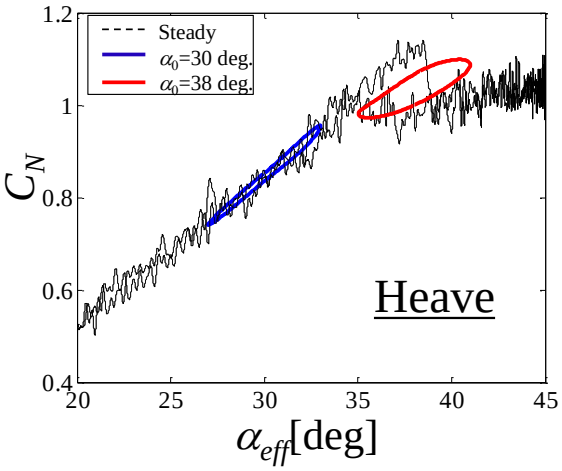

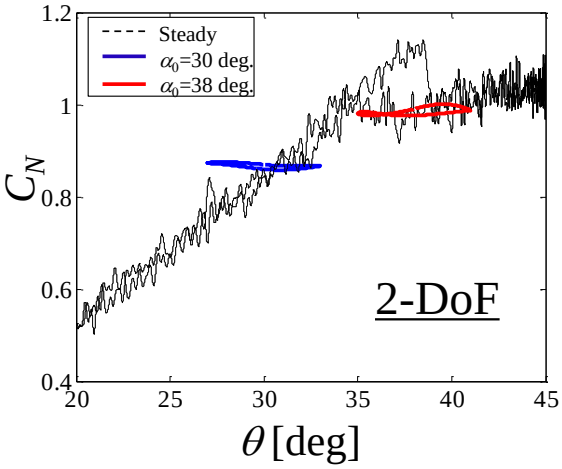

Fig. 14 Effects of model motion on unsteady normal force coefficient, for k = 0.024 and $\Delta\alpha_{\text{eff}}$ ($\Delta\theta$ for 2-DoF case) = 3 deg.